Supplementary Information for:

Contributions of biogenic material to the atmospheric ice-nucleating particle population in North Western Europe

D. O'Sullivan,[1] M.P. Adams,[1] M.D. Tarn,[1] A.D. Harrison,[1] J. Vergara-Temprado,[1] G.C.E. Porter,[1] M.A. Holden,[1,2] A. Sanchez-Marroquin,[1] F. Carotenuto[3], T.F. Whale[1], J.B. McQuaid[1], R. Walshaw,[4] D.H.P. Hedges,[4] I.T. Burke,[5] Z. Cui[1] and B.J. Murray[1]

[1] Institute for Climate and Atmospheric Science, School of Earth and Environment, University of Leeds, Woodhouse Lane, Leeds, LS2 9JT, UK

[2] School of Chemistry, University of Leeds, Woodhouse Lane, Leeds, LS2 9JT, UK

[3] Institute of Biometeorology, National Research Council (IBIMET-CNR), Via Caproni 8, 50145 Florence, Italy

[4]School of Earth and Environment, University of Leeds, Woodhouse Lane, Leeds, LS2 9JT, UK

[5]Earth Surface Science Institute, School of Earth and Environment, University of Leeds, Woodhouse Lane, Leeds, LS2 9JT, UK

Corresponding Author: Benjamin Murray Email: b.j.murray@leeds.ac.uk Tel: +44 (0)113 343 5605. Institute for Climate and Atmospheric Science, School of Earth and Environment, University of Leeds, Woodhouse Lane, Leeds, LS2 9JT, UK

Supplementary tables and figures

	Total number of runs = 51	
	Run Time (min)	**Volume air sampled (L)**
Average	178	888
Max	433	2165
Min	60	300

SI Table 1: Sampling times and volume of air sampled for the 51 runs performed during the campaign.

Start	End	$INP_{-25°C}$	$INP_{-20°C}$	$INP_{-15°C}$	Runtime	Vol. air sampled
			#/ L		*(min)*	*(L)*
26/09/2016 12:00	26/09/2016 15:00		0.6		180	900
26/09/2016 12:11	26/09/2016 15:12		0.4		181	905
27/09/2016 10:57	27/09/2016 14:26		0.6	0.2	209	1045
28/09/2016 12:35	28/09/2016 15:35		0.5		180	900
28/09/2016 13:34	28/09/2016 15:40			3.3	126	630
30/09/2016 10:19	30/09/2016 13:19		0.7		180	900
30/09/2016 11:20	30/09/2016 13:55		0.8		155	775
30/09/2016 14:21	30/09/2016 16:21		1.0		120	600
03/10/2016 10:20	03/10/2016 13:59	8.4			219	1095
03/10/2016 10:26	03/10/2016 13:27	7.9			181	905
03/10/2016 10:32	03/10/2016 13:35		0.5	0.2	183	915
03/10/2016 13:35	03/10/2016 16:36		1.8		181	905
03/10/2016 13:47	03/10/2016 16:23			1.2	156	780
04/10/2016 10:33	04/10/2016 13:20	12.3	2.8		167	835
05/10/2016 11:16	05/10/2016 12:18	17.7			62	310
05/10/2016 11:16	05/10/2016 15:59		11.4		283	1415
05/10/2016 13:39	05/10/2016 14:39		11.1		60	300
06/10/2016 11:39	06/10/2016 14:13		1.3		154	770
06/10/2016 11:40	06/10/2016 14:10	3.4	0.2		150	750
06/10/2016 14:20	06/10/2016 16:58		3.9		158	790
06/10/2016 14:24	06/10/2016 16:54		4.0		150	750
07/10/2016 10:41	07/10/2016 12:41		1.6		120	600
07/10/2016 11:21	07/10/2016 13:06			0.4	105	525
07/10/2016 13:02	07/10/2016 15:02	14.2	0.8		120	600
10/10/2016 11:29	10/10/2016 16:36		0.5		307	1535

10/10/2016 12:39	10/10/2016 13:39		1.9		60	300
10/10/2016 13:50	10/10/2016 16:36		0.4		166	830
11/10/2016 10:40	11/10/2016 14:03	10.0	0.6		203	1015
11/10/2016 14:10	11/10/2016 16:24	16.3	8.4		134	670
13/10/2016 10:39	13/10/2016 14:42		1.3		243	1215
13/10/2016 10:41	13/10/2016 14:42		0.9		241	1205
14/10/2016 07:30	14/10/2016 10:31			1.2	181	905
14/10/2016 10:39	14/10/2016 12:19		3.9	0.7	100	500
17/10/2016 11:46	17/10/2016 14:49		1.1		183	915
17/10/2016 15:10	17/10/2016 17:11	25.1	5.8		121	605
18/10/2016 10:45	18/10/2016 13:52		2.1	0.2	187	935
18/10/2016 10:55	18/10/2016 14:15	12.6	0.4		200	1000
18/10/2016 10:55	18/10/2016 16:10		0.3		315	1575
18/10/2016 14:00	18/10/2016 16:15		1.2	0.4	135	675
18/10/2016 14:15	18/10/2016 16:10	18.5	2.7		115	575
19/10/2016 10:04	19/10/2016 13:04		21.7	0.9	180	900
19/10/2016 13:20	19/10/2016 16:21		1.1	0.3	181	905
20/10/2016 11:45	20/10/2016 13:35	8.8			110	550
20/10/2016 13:45	20/10/2016 16:00	8.6			135	675
21/10/2016 11:42	21/10/2016 16:36		2.6	2.0	294	1470
21/10/2016 14:42	21/10/2016 16:36		4.1	3.9	114	570
24/10/2016 12:05	24/10/2016 15:37		1.6		212	1060
27/10/2016 11:49	27/10/2016 15:58	13.7	3.8	1.3	249	1245
31/10/2016 10:17	31/10/2016 17:30	6.8	0.4		433	2165
01/11/2016 11:10	01/11/2016 14:10	3.2			180	900
02/11/2016 10:29	02/11/2016 15:29		0.2		300	1500

SI Table 2: Extended data for the sampling periods

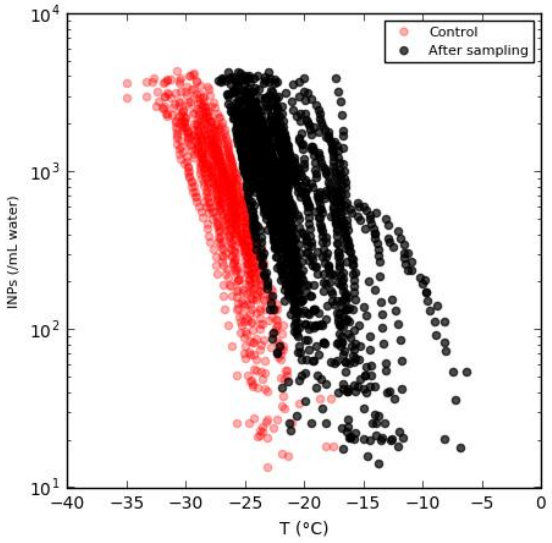

SI Fig 1: Data indicating the levels of INPs before and after sampling in the Milli-Q water. On any given day, INPs in the background were typically an order of magnitude less than those after sampling.

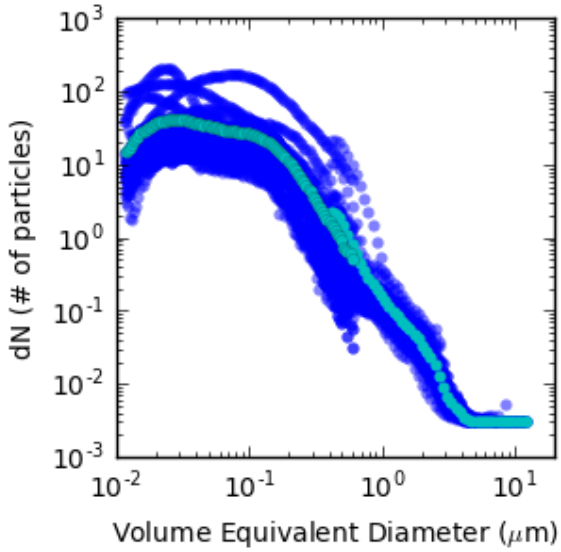

SI Fig 2: Compilation of aerosol particle size distributions measured throughout the campaign. The merged APS and SMPS measurements are shown in dark blue, while the average of all of these is shown in cyan.

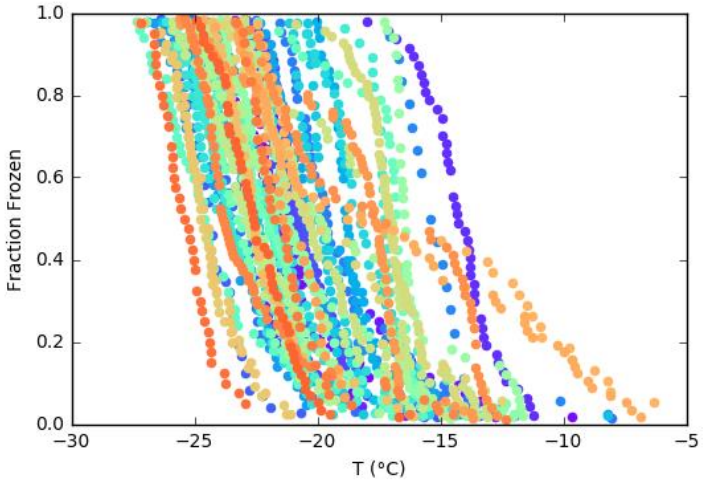

SI Fig 3: Compilation of all the experimental fraction frozen curves for the samples collected during the campaign.

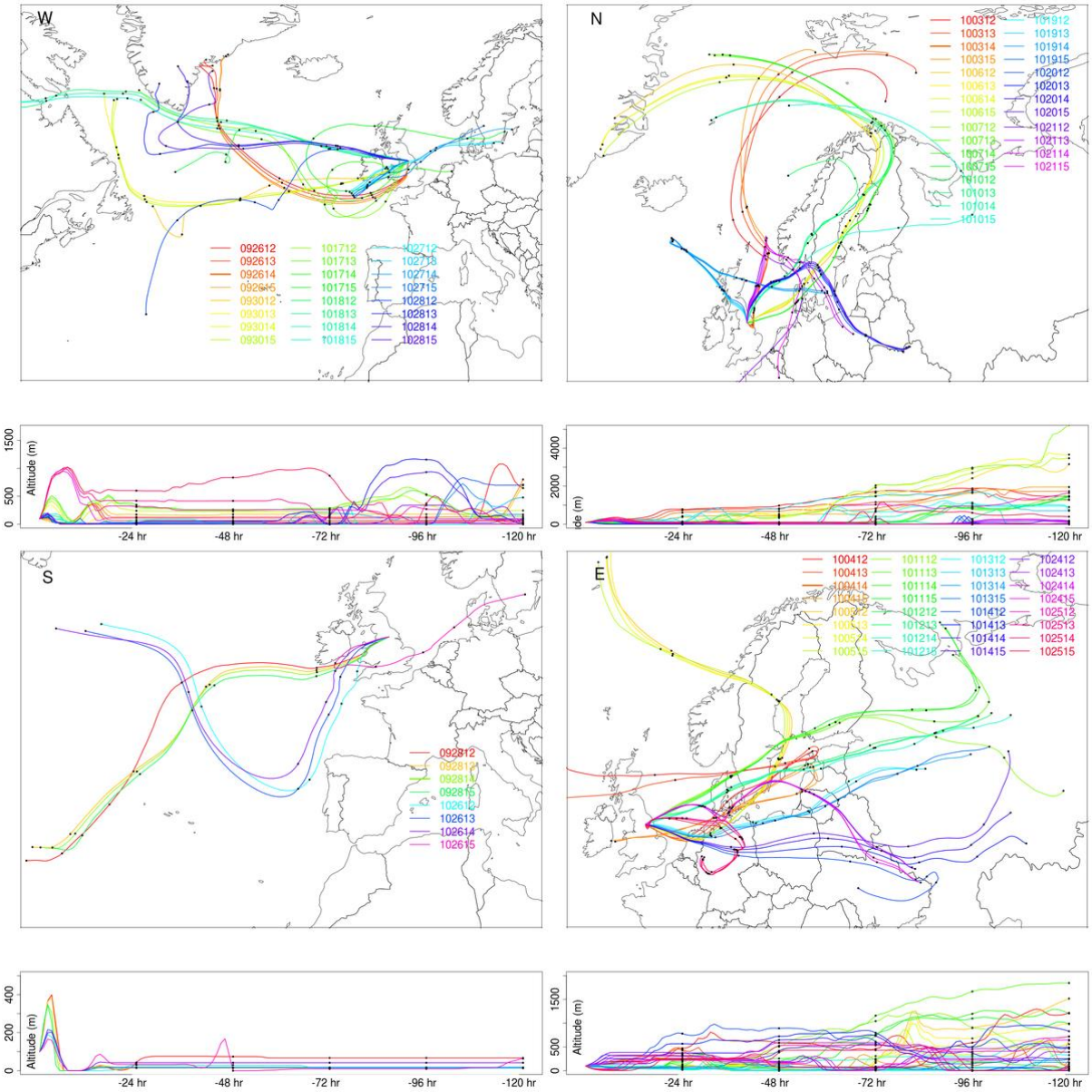

SI Fig 4: HYSPLITT back trajectory profiles. The letter in the top left corner indicates the assigned predominant direction for the trajectory which was used for the analysis in Fig 3 of the main paper. The trajectories are taken every hour during the sampling periods, and the altitudes of the back trajectories are in the panels beneath the main graph.

SEM- EDS analysis

Scanning electron microscopy was used to directly analyse the morphology and composition of the aerosol particles on one of the filters collected during the campaign (17th October 2016). A similar approach has been used in Chou et al.,[1] Hand et al.[2] and Young et al.[3] The polycarbonate filter was analysed using a Tescan VEGA3 XM scanning electron microscope (SEM) fitted with an X-max 150 SDD energy-dispersive X-ray spectroscopy (EDS) system controlled by AZtec 3.3 software. Prior to analysis, the filter was coated with iridium (30 nm) in order to make the filter substrate conductive. The SEM was operated at 20 keV, using a beam spot size that was adjusted to provide the optimum number of input counts for the EDS detector and a working distance of around 15 mm, with a Secondary Electron detector. Particle size, shape and compositional data was collected using the "AZtecFeature" software, optimised for particle analysis, as described below. Randomly chosen areas on the filter were scanned (avoiding being close to the filter edges) at two different magnifications, with a dwell time of 10 µs and a resolution of 1024 x 960 pixels per image. High magnification images (normally x5000) were used to detect particles down to 0.2 µm and medium magnification images (normally x1500) were used to scan particles down to 1 µm. Particles were identified based on their relative brightness compared with the background filter. The brightness threshold was determined manually for each area, in order to detect most of the small particles and minimize artefacts (primarily bright spots present at the edges of filter pores). The AZtecFeature software calculates the size and shape of each particle. Data was then expressed as the equivalent circular diameter of each particle which is defined as $\sqrt{(4A/\pi)}$, where A is the cross sectional area of the particle.

EDS spectra were collected from the centre of some of the first particles detected in each area. The number of counts obtained per particle was around 50,000. From the X-ray spectrum of each particle, elemental weight percentages were calculated by the AZtecFeature software, and then used to categorise the particles into different compositional bins. Because of the fact that the

interaction volume (~2-5 μm^3) is in most cases larger than the particle volume, the X-ray spectra of each particle also contains peaks due to X-rays emanating from the polycarbonate filter, which is made of carbon and oxygen. As a consequence, the elemental weight percentages of the elements present in the particle would not correspond to the weight percentages obtained by the EDS analysis. Therefore, when categorising particles based on their composition, only the presence or absence of elements and the ratio between different elements was taken into account (see full scheme in SI Table 3). The compositionally categorised particles were then presented as the fraction of particles present in each category bin at each size bin (see SI Fig 5). In addition, we manually searched the filter for particles which were of obvious biological origin. These particles are shown in SI Fig 6 and are most likely fungal spores.

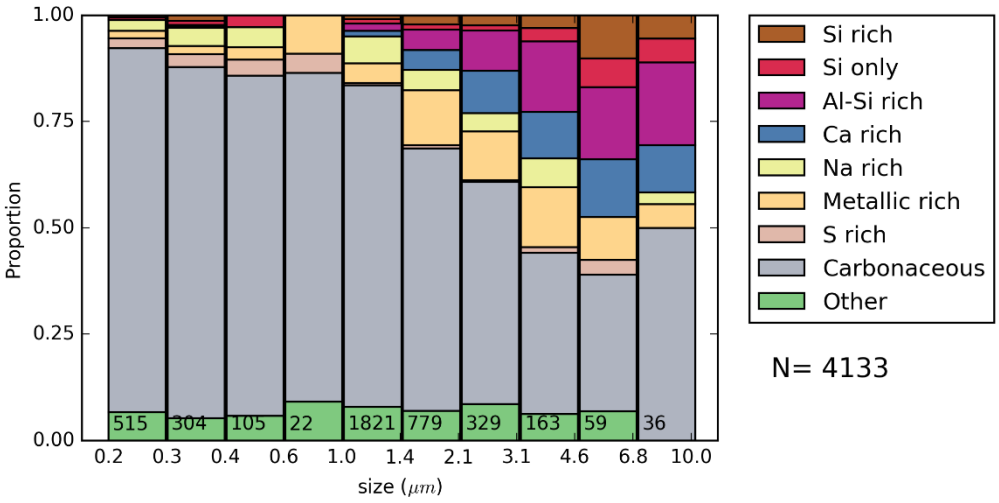

SI Fig 5: Size-resolved SEM-EDS analysis of a filter collected on 17th October 2016, showing the fraction of particles belonging to each compositional category for each size bin according to their EDS spectra and equivalent circular diameter. A description and interpretation of the bins appears in SI Table 3. The most abundant group is carbonaceous particles, consistent with organic and black carbon particles. There is a significant contribution from Na and Cl rich particles (likely as NaCl) and metallic aerosol particles. The vast majority of particles in the categories Al-Si rich, Si only and Si rich are consistent with mineral dust. By summing these bins together, a mode of mineral dust can be seen in the supermicron size. The number of particles per bin is shown in the bottom of the bar. The total number of particles is also shown (N).

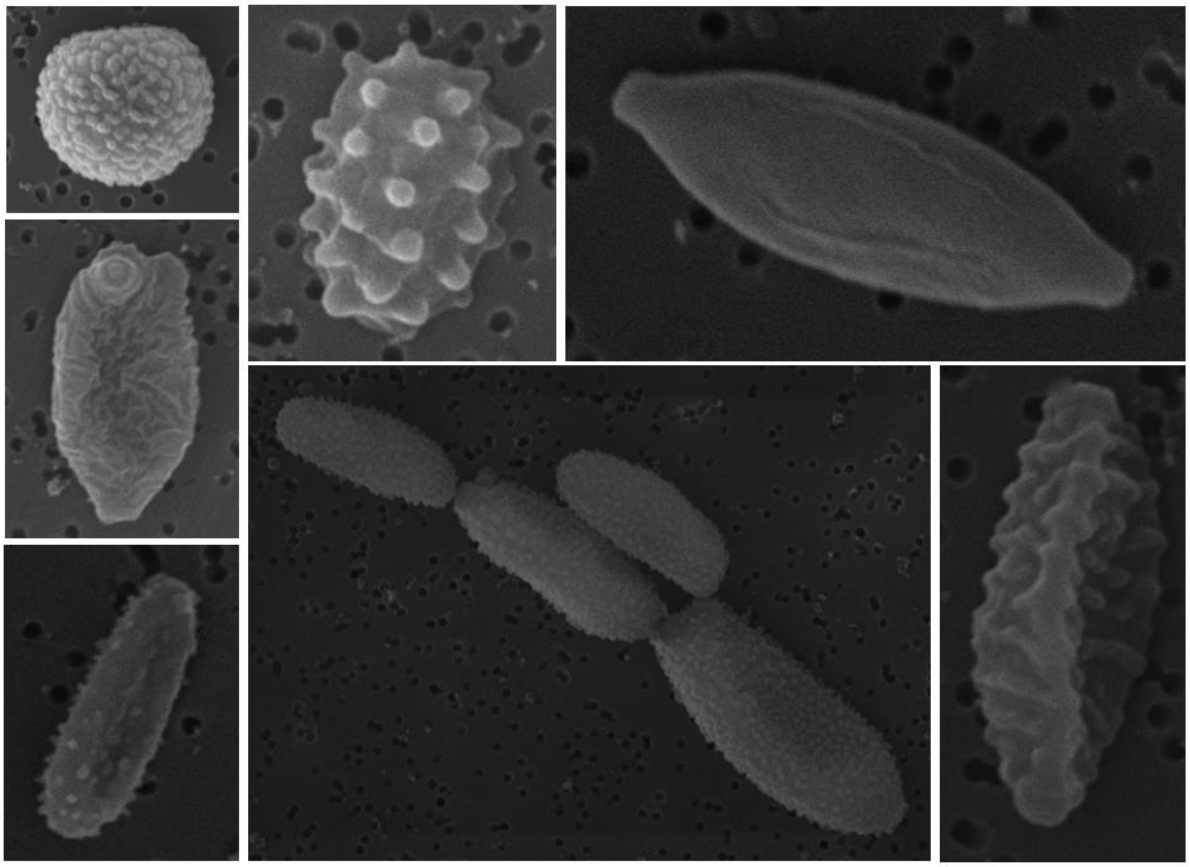

SI Fig 6: Scanning electron microscope images of a selection of particles which were obviously biological. These particles appear to be various types of fungal spore. The images demonstrate the presence of biological particles at the sampling site, but the statistics were poor and hence it was not possible to quantify their concentration. In addition, we were only able to identify biological particles by visual inspection, hence we most likely miss biological fragments and other biogenic-containing aerosol particle types. These particles fall into the carbonaceous category in SI Fig 5. For scale, the small black pores in the filter in the background of each image are 0.4 µm diameter.

Category	Primary	Secondary	Interpretation
Carbonaceous	C+O	C+O C+O+K C+O+P	• black carbon, organic, biogenic
S rich	S		• sulphates
Metal rich	Fe/Al/Cr/Zn/Ti		• metal oxides, metal rich aerosol
Na rich	Na	Na+Cl Na+Cl+(Mn, Mg) Na+Cl+S	• sea salt, aged sea salt
Al-Si rich	Al/Si	Al+Si Al+Si+(Na, Mg, K, Ca, Fe, S)	• aluminosilicates
Ca rich	Ca	Ca Ca+S Ca+(Al, Si, Na, Mg, K, Ca, Fe)	• calcium carbonate, gypsum, Ca-rich mixed particles
Si only	Si		• silica
Si rich	Si	Si+(Na, Mg ,K, Ca, Fe)	• internally mixed silica, silicates
Other	Mixture	Mixture	• internally mixed particles, particles where the categorisation failed

SI Table 3: Primary and secondary elements present each category and interpretation of the most likely type of aerosol. Secondary elements in parenthesis mean that at least one of the listed elements in the parenthesis was detected. C and O were present in the EDS spectra of all particles, so it is not mentioned after the first category. Due to the spatial resolution of the EDS, C and O were identified in each case from the polycarbonate filter, but may also have been present in the other aerosol particle types as black carbon, biogenic species, and as a component of organic and inorganic molecules (e.g. $CaCO_3$).

References

1. Chou, C. *et al.* Size distribution, shape, and composition of mineral dust aerosols collected during the African Monsoon Multidisciplinary Analysis Special Observation Period 0: Dust and Biomass-Burning Experiment field campaign in Niger, January 2006. *J. Geophys. Res. Atmos.* **113**, D00C10 (2008).

2. Hand, V. L. *et al.* Evidence of internal mixing of African dust and biomass burning particles by individual particle analysis using electron beam techniques. *J. Geophys. Res. Atmos.* **115**, D13301 (2010).

3. Young, G. *et al.* Size-segregated compositional analysis of aerosol particles collected in the European Arctic during the ACCACIA campaign. *Atmos. Chem. Phys.* **16**, 4063–4079 (2016).